Available online at www.sciencedirect.com

ScienceDirect

Energy Procedia 69 (2015) 369 – 378

Energy Procedia

International Conference on Concentrating Solar Power and Chemical Energy Systems, SolarPACES 2014

Development of insulation for high flux density receivers

M. Ebert[a]*, W. Arnold[b], A. Avila-Marin[c], T. Denk[d], J. Hertel[a], A. Jensch[a], W. Reinalter[e], A. Schlierbach[e], R. Uhlig[a]

[a]German Aerospace Center (DLR), Institute of Solar Research, Pfaffenwaldring 38-40, 70372 Stuttgart, Germany
[b]EUGEN ARNOLD GmbH, Carl-Zeiss-Straße 14, 70794 Filderstadt-Harthausen, Germany
[c]Plataforma Solar de Almería - CIEMAT, Avda. Complutense 40, Madrid E-28040, Spain
[d]Plataforma Solar de Almería - CIEMAT, Ctra. de Senés, s/n, 04200 Tabernas, Spain
[e]German Aerospace Center (DLR), Institute of Solar Research, Ctra. de Senés, s/n, 04200 Tabernas, Spain

Abstract

In the last years more experience has been achieved with long time operation of solar tower receivers increased in size. The insulation of these receivers shows higher complexity and importance compared to small prototypes [1, 2]. Both insulation of tubular cavity receiver and inner insulation of piping are safety-relevant components as they protect e.g. support structures and pressurized tubes and connections against overheating. Besides safety, operating reliability is one of the most important requirements to meet as down times, maintenance and repairs cause high costs.
This paper describes the new development of the insulation for a tubular cavity receiver with air as heat transfer medium, where costs and thermal heat loss should be reduced. The prototype has been designed, built and tested for 100 operating hours at receiver outlet temperatures of up to 800°C at the test facility Plataforma Solar de Almería (PSA), Spain. The results of a thermal model, of material tests and the evaluation of the thermal heat loss are presented.

Peer review by the scientific conference committee of SolarPACES 2014 under responsibility of PSE AG

Keywords: cavity receiver; insulation, solar tower, micro turbine system

* Corresponding author. Tel.: +49-711-6862-626; fax: +49-711-6862-.
E-mail address: miriam.ebert@dlr.de

Peer review by the scientific conference committee of SolarPACES 2014 under responsibility of PSE AG
doi:10.1016/j.egypro.2015.03.043

1. Introduction

In the last years more experience has been achieved with long time operation of solar tower receivers increased in size. The insulation of these receivers shows higher complexity and importance compared to small prototypes [1, 2]. Special load conditions like inhomogeneous and fluctuating solar flux and a dusty and humid ambient need to be considered. Both insulation of tubular cavity receiver and inner insulation of piping are safety-relevant components as they protect e.g. support structures and pressurized tubes and connections against overheating. Besides safety, operating reliability is one of the most important requirements to meet as down times, maintenance and repairs cause high costs. Additionally, high performance, that means low heat losses, and low costs need to be achieved for commercialization of these systems [3].

Nomenclature

$A_{surface}$	inner cavity surface area
h_{inlet}	enthalpy of air at receiver inlet
h_{outlet}	enthalpy of air at receiver outlet
$h_{insulation}$	heat transfer coefficient though insulation
$\dot{m}_{air}$	air mass flow of receiver
$Q_{heat\ loss}$	heat loss
T_{inlet}	temperature at receiver inlet
T_{outlet}	temperature at receiver outlet

On cavity receivers like shown in Figure 1 the cavity consists of an insulated housing with the function of reducing thermal losses of the receiver. It also protects all components except the receiver from concentrated solar radiation. Another important effect is the homogenization of the solar flux density by reflecting the solar radiation on the cavity walls. The development of a new design of such insulation and its test and evaluation is presented hereafter.

In a first step a parametric theoretical model was created to evaluate geometry influence on the performance. This model presented in 2.1 is based on a tubular receiver to be installed in Brazil in the framework of the project SMILE, whereas the later manufacturing and testing of the insulation prototype was realized for an already existing micro-turbine system at Plataforma Solar de Almería in Spain. The scheme of this system developed in the former EU project SOLHYCO [4] is shown in Figure 1. It uses the same micro-turbine as in the SMILE project but the receiver geometry is slightly different.

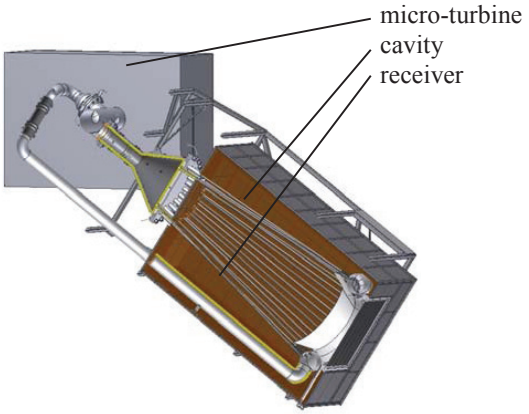

Fig. 1. scheme of a tubular cavity receiver with a micro turbine, project SOLHYCO

2. Design

The design of the insulation is subject to different requirements like geometrical restrictions, costs and targeted heat losses and material temperatures. For a basic design of the geometry a three dimensional fully parametric thermal finite element-model (FEM) was developed to be able to evaluate the influence of the cavity geometry on the receiver performance.

As the receiver dimension and heliostat field design are already fixed, the length of the cavity (3.24m), the minimum diameter (2.4m) and the diameter of the aperture (0.8m) are predetermined. The parameters to be modified are the shape of the cavity (cylindrical, conically tapered to the inlet or outlet and polygon with different numbers of corners) and the diameter.

The selected receiver for the model consists of a bundle of 86 cylindrically arranged parallel tubes.

2.1. Thermal model

The model is based on a tool developed by DLR that combines the incoming solar radiation from the heliostat field using a ray-tracer with the receiver model implemented in a commercial FEM solver. The so called FEMRAY code (Finite Element Mesh Ray Tracing [5]) calculates the incoming heat flux distribution on the receiver and the insulation. It considers input data like geometry, position and orientation of the heliostats, location of the plant, date and time of the evaluation and optical properties of the materials.

In the thermal model absorption, reflection and radiation on the surfaces of the insulation and the receiver are considered. Heat transfer coefficients given by Nusselt correlations are applied for to calculate the heat transfer inside the tubes to the fluid. For the convection from the cavity walls to ambient a validated correlation from literature is used.

The input parameters are given in Table 1.

Table 1. Input parameters of geometric model

Input parameters	value	Units
Absorption coefficient for absorber tubes at solar wavelength	0.9	-
Absorption coefficient for insulation at solar wavelength	0.3	-
Absorption coefficient for absorber tubes at infrared wavelength	0.9	-
Absorption coefficient for insulation at infrared wavelength	0.5	-
Heat conductivity insulation at design point	0.1	W/m*K
Heat transfer coefficient fluid flow absorber tubes	335	W/m²*K
Heat transfer coefficient insulation to ambient	0.2	W/m²*K
Heat transfer fluid pressure	10	bar
Heat transfer fluid inlet temperature	600	°C
Heat transfer fluid mass flow	0.8	kg/s
Ambient temperature	25°C	°C
Ambient temperature inside tower	60°C	°C
Date and time	032112	MMDDHH

Figure 2a shows the different efficiencies of the receiver system where the optical efficiency only considers losses due to reflection out of the aperture of the cavity whereas the thermal efficiency considers losses due to conduction through the cavity walls and convection and radiation through the aperture. As expected, optical efficiency increases with bigger cavities, i.e. higher ratio between cavity diameter and aperture diameter due to higher reflection inside of the cavity. Increasing the size of the cavity from 2m to 5m leads to an increase of the optical efficiency from 98.3% to 99.3% for a cylindrical cavity.

Nevertheless compared to this small difference in optical efficiency a significant decrease in thermal efficiency can be observed. Figure 2b depicts the variation of the different heat loss mechanisms and additionally the total inner surface of the cavity with increasing diameter. While the reflected solar radiation through the aperture halves and radiation to ambient nearly keeps the same, convection and conduction losses triplicate both with an even higher increase of the cavity area.

Besides high efficiency the design should meet requirements for the technical feasibility. Particular attention should be paid to maximum material temperatures as this influences costs and life expectancy. By increasing the cavity dimensions and thus decreasing and homogenizing the flux density on the insulation the model shows that the maximum inner surface temperature of the insulation only drops from 900°C to 875°C.

No significant differences in values and trends for conically tapered or polygon shape cavities compared to cylindrical shaped cavities can be observed.

As demonstrated, the negative impact on the thermal efficiency of a bigger cavity exceeds by far the positive effects like optical efficiency and lower material temperatures. Additionally material costs rise with the needed area. Therefore, the main focus during the design of the insulation was put on cost and manufacturing aspects.

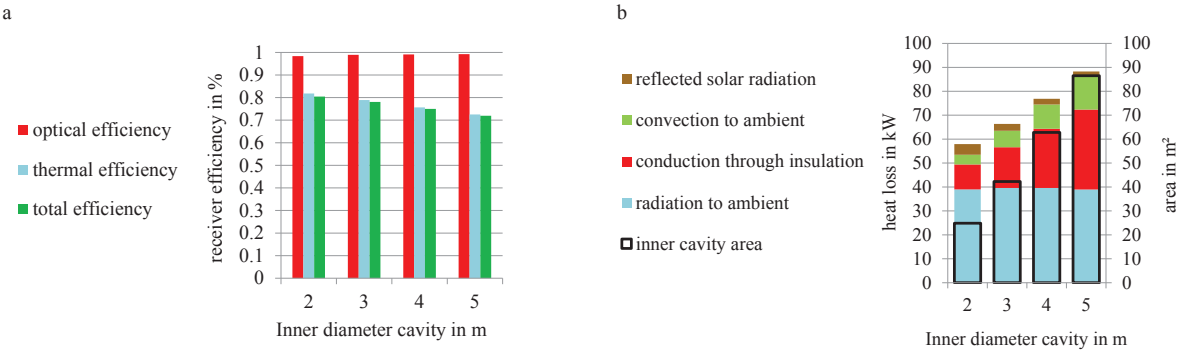

Fig. 2. (a) efficiencies and (b) losses and surface area for different cavity diameters, cylindrical shape

2.2. Design and construction

As a result of 2.1 a dodecagon was chosen for the cavity design. This shape needs less material than a polygon with fewer corners and can be built of flat, modular elements that allow an easier manufacturing and assembling and therefore lower costs than a cylindrical shape. In circumferential direction the dodecagon is divided in six insulation cassettes and in longitudinal direction in two cassettes like shown in Figure 3. A division in several segments is needed to allow thermal expansions.

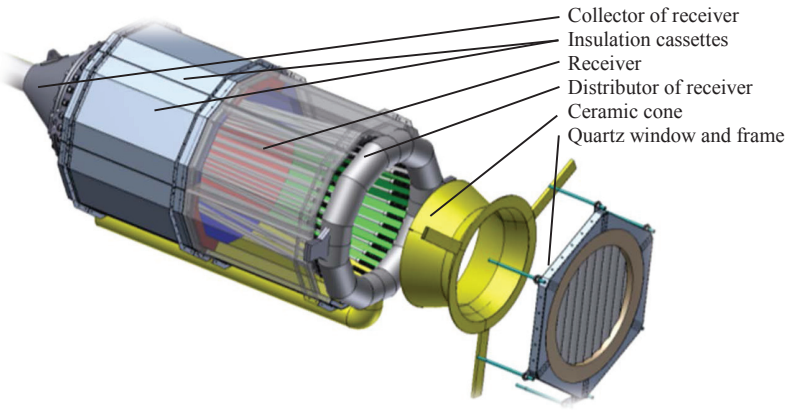

Fig. 3. Exploded view of the insulation and the receiver

Each cassette has a metallic back structure encapsulating the insulation material. The insulation material located on the inside consists of a combination of two different ceramic fiber types. The cassettes are arranged in an overlapping formation to avoid gaps due to material shrinking and thermal expansions. Additionally, the irradiated side of the insulation is covered by a ceramic fiber fabric. The cassettes are sized to fit into an elevator for transport.

The back part of the insulation is firmly connected to the receiver collector. The insulation is mounted on six steel cables connected to the supporting structure. This allows a flexible movement of the insulation following the linear expansion of the receiver tubes. The absorber tubes need to be fed through the insulation. As explained in 3.1 several solutions were tested resulting in a layered approach: an SIO2 braided fiberglass tape is wrapped around the absorber tube. The wrapping is additionally overlapped by insulation pillows consisting of silica glass fabric filled with fiber material to avoid that radiation is transmitted through gaps.

The receiver's distribution ring is packed with flexible insulation material similar to the pillows described above and protected against direct solar radiation with an additional ceramic cone.

To reduce heat losses a quartz window [6] should be optionally installable. Therefore a window frame is located at the receiver aperture to operate the receiver with and without the window. The window consists of ten sixth-tube segments which are arranged side by side. All segments are mounted in a frame made of milled boards of vermiculite that is cased in a metallic structure. The window frame is fixed on a threaded rod which is connected to the cavity. Flexible insulation material is used between the window and the front protection of the tower to ensure radiation tightness.

The design process was supported by FEM calculations, analyzing receiver frame and support structure with regard to thermal expansion and material stress.

3. Manufacturing and mounting

3.1. Materials

Material testing has been conducted with the main focus on applicability for the insulation of the test receiver cavity. The following boundary conditions for the insulation materials resulted from the insulation design: application temperature of above 1000°C, high insulation properties in order to minimize heat losses to less than 15kW, no particle emission from the insulation, material strength at high temperatures (alternating mechanical loads due to strains and deformations of the cavity insulation) and flexibility allowing passageways for metallic components like absorber tubes and the receiver mounting.

The test stand was comprised of exchangeable insulated walls and an absorber tube and heated by a 10kW infrared heater. With this type of design, both insulation materials and the feed through solutions for the absorber tube could be tested.

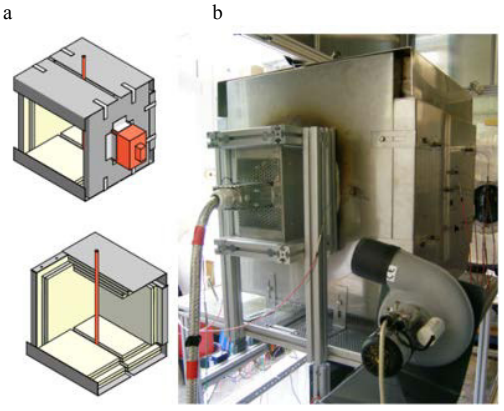

Fig. 4. (a) drawing of the test stand; (b) picture of the test stand

Insulation material chosen was high temperature silica fiber with a classification temperature† of 1300°C [8] and good machinability. The fibers are highly bio soluble and therefore not classified as hazardous. Several layers of the material, compressed into blocks, were glued together to a stack and then also glued to the stainless steel back structure with ceramic adhesive – this being a very simple and hence low cost manufacturing option imaginable for application in the cassettes of the insulation. Cyclic testing was conducted within the test stand with maximum temperatures of about 800°C on the hot side of the insulation material. The gluing connection proved insufficient with the insulation fibers tearing out at the glue connection. The alternative connection method of connecting the boards of insulation material using bayonet bolts did not show these problems within the first hours of testing. However, more testing hours are necessary for reliable conclusions.

Further efforts were made to test solutions for the passageway of metallic components through the insulation material. The first solution option, sewn pillows made of woven ceramic fiber fabric filled with insulation material, has several advantages: with the sewing process a wide variety of shapes is feasible and the fabric itself has a very high flexibility. Testing the fabric material in a furnace at 1000°C showed no signs of wear (embrittlement). However, the manufacturing process is limited in precision and minimal size of patterns. Filling gaps with loose fiber materials would be necessary (Figure 5a) so that this solution could be less reliable in operation. The second option consisted of a ceramic fabric tape, wound around the tube and fastened with wire made of high temperature alloys. Tests showed that it is possible to wind the tape by hand tight enough around the tube that the connection will transmit almost no light (Figure 5b). Repeated cycling showed that the binding will loosen slightly after several cycles (Figure 5c) of tube expansion and contraction but still be tight enough for the application.

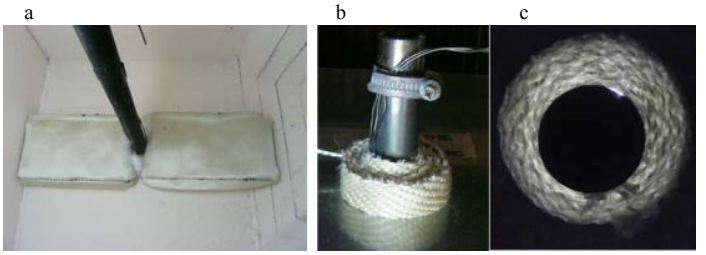

Fig. 5. (a) sewed pillows with absorber tube feed trough; (b) winded ceramic fabric tape; (c) tape after cycling

3.2. Manufacturing

As described in 2.2 single metal sheet cassettes are filled with two different ceramic fiber types. Black plastic tapes visible in Figure 6a and b are used to compress the insulation layers in order to ensure a homogenous insulation material density over the entire cassette. At last the insulation module is covered with a high temperature durable glass fiber fabric (Fig. 6c). After manufacturing the individual modules, the cavity was preassembled like shown in Figure 6d on manufacturer site to check all components.

† The classification temperature is defined as the temperature at which a linear shrinkage of 4% is not exceeded after 24 hour heat treatment in the electrically heated laboratory oven and in a neutral atmosphere.

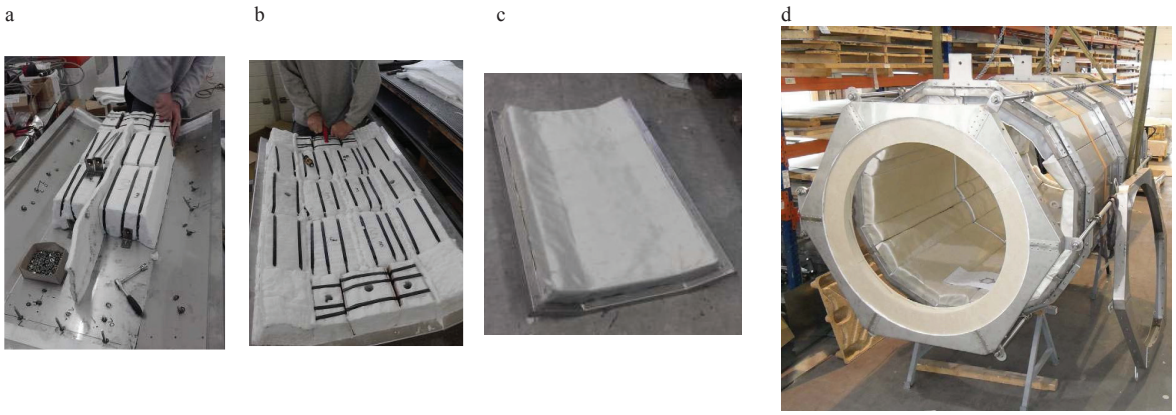

Fig. 6. (a) layer of insulation material; (b) insulation before taking off the compression tape; (c) completed cassette covered with ceramic fabric; (d) preassembled cavity

3.3. Installation at PSA

Installation sequence of the modularly built-up insulation system started at the distributor, shown in Figure 7a. Subsequently the individual cassettes were placed and connected to each other forming a cylindrical casing. This part was fixed to the support before installing the ceramic cone and the top end with the feed-through of the absorber tubes. The alignment of the cavity to the receiver as the following step is important to guarantee the same course of movement of both elements.

After the positioning process the cylindrical isolation was fixed to the back part of the cavity which had been sealed with insulation pillows and the absorber tubes were lagged with ceramic fabric tape to achieve an irradiance tight closure (Figure 7b). Gaps at the hems between the cassettes and pillows were tightened with loose ceramic material.

After finishing the inner part of the cavity the section around the aperture was installed. All absorber tube compensators were individually insulated. The ceramic cone consisting of three parts was mounted around the distributor and the window frame installed (Figure 7c). At last the intersection between cavity and tower was adapted to provide an irradiance tight insulation. A view from the front side of the aperture is given in Figure 7d.

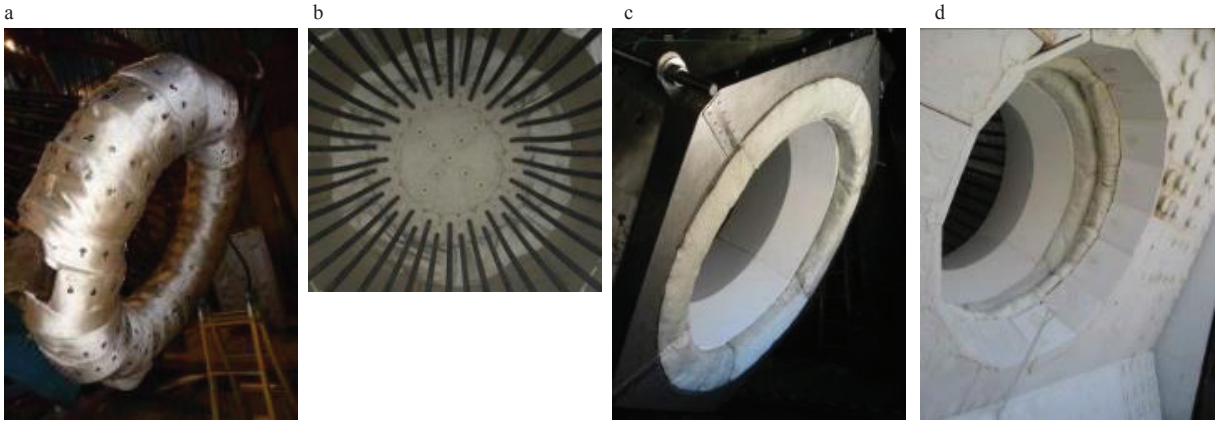

Fig. 7. (a) insulated distribution ring; (b) finished cavity rear panel; (c) window frame and cone at distributor ring; (d) system in operation position view from outside the tower

4. Tests

Test set up for the new insulation system was the existing micro gas turbine system (Project SolHyCo) at 60m on the CESA1 solar tower at PSA. Unfortunately, the turbine had a defect and could not be fixed within project time limits due to internal changes of the owner company. As an alternative, a blower providing the air mass flow for the receiver was integrated at the receiver inlet. As fluid properties like pressure and receiver inlet temperature therefore changed, the determination of the overall efficiency of the system was not possible anymore.

To test and evaluate the new insulation the system was operated increasing the receiver outlet temperature step by step over the test period by increasing solar input power. Before starting these solar tests and after each temperature level a non-solar test was carried out to determine the heat transfer through the cavity walls. Therefore the receiver, and thus the cavity, was heated up excluding convection and radiation losses through the aperture by closing it with an insulated plate. Thus, only heat loss by conduction though the insulation wall is left and can be calculated by drawing the energy balance of the receiver. The required heat source was provided by an air heater installed between blower and receiver inlet. Maximum achieved air inlet temperature with the heater was about 300°C.

The new insulation's functionality was tested in solar load tests increasing receiver outlet temperatures in 100K steps up to 800°C. Heat loss tests were repeatedly realized every 10-15 solar operation hours after every temperature level rise to be able to identify a potential change in characteristic.

5. Results and outlook

5.1. Observation

During the solar tests from January 2014 until March 2014 more than 100 solar operating hours have been achieved. Figure 8a shows the distribution of hours versus the outlet temperature of the absorber tubes of the receiver.

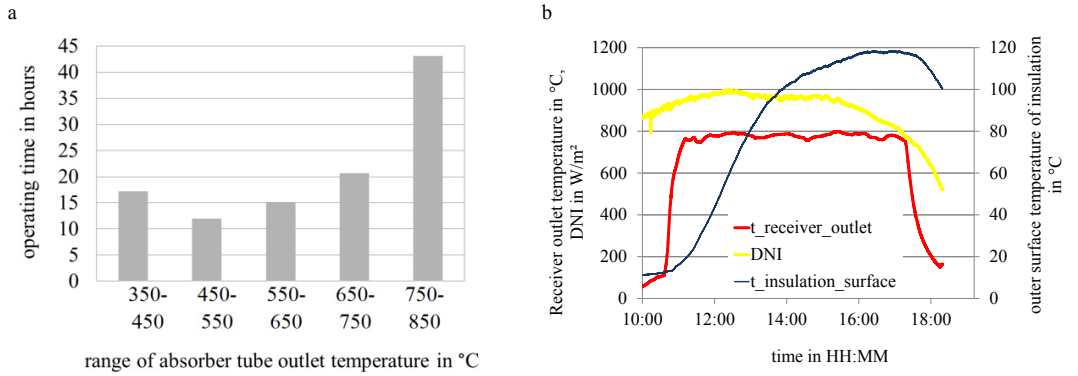

Fig. 8. (a) operating hours vs. absorber tube outlet temperature; (b) outer surface temperature of insulation at maximum receiver outlet temperatures

Even though the tested materials are supposed to withstand temperatures up to 1300°C, the material indicated failure after the short operation time and had become very porous. This shows, that high solar fluxes with inhomogeneous and fluctuating thermal loads result indistinctively higher and more complex strains on the materials than merely high temperatures. The junction between the cassettes foreseen for thermal expansion extended each time increasing the thermal load. After solar operation the cassettes did not move back to their original position and a gap appeared. Figure 8b shows the outer surface temperatures of the cavity at maximum operation temperatures of 800°C after 90 solar operation hours on March 10th 2014. Temperatures rose beyond 120°C.

The loose ceramic material which had been used to fill the gaps started to fall out already after first solar operation. Other than in most commercial oven applications shrinking material falling out cannot easily be replaced due to bad accessibility. Therefore maintenance has to be kept at a minimum through prevention.

5.2. Determination of thermal heat losses

As explained in capture 4 the heat loss $Q_{heat\ loss}$ corresponds to the energy balance of the receiver with closed aperture and can be calculated by the enthalpy difference h_{outlet} -h_{inlet} of the heated air between the inlet and the outlet of the receiver when steady state conditions are reached and storage term disappears in the energy balance (1).

$$Q_{heat\ loss} = \dot{m}_{air} * \left(h_{outlet} - h_{inlet}\right) \quad (1)$$

The enthalpy flow was calculated using the signals of an absolute system pressure sensor and a pitot tube sensor for the air mass flow $\dot{m}_{air}$ both installed in the inlet pipe close to the entrance into the cavity (see [1] for detailed system description). A PT100 sensor provided with the mass flow device was used for the inlet temperature and the outlet temperature was determined by the average of the absorber tube outlet temperatures with one thermocouple installed at the end of each tube. Four of the 40 sensors had to be excluded from the calculation because of wrong or unreliable signals. Using the average outlet temperature neglects different mass flow through the single absorber tubes that might be caused by a different pressure drop in each tube and also neglects the effect of the different temperatures (ΔT between tubes < 15K for steady state conditions) on the viscosity of the air. Steady state conditions were reached heating the air with the electrical pre-heating during many hours to about 300°C.

The figures below show the evolution of the heat loss as a function of the solar operation time (Figure 9a) and of the maximum operation temperature the system was exposed before the test (Figure 9b).

As it can be observed, heat loss increased significantly from 5kW before the first solar test up to approximately 6kW after 19 h of solar operation. Heat loss then continued to increase, however less severely, with operation time and temperature. These results correspond to the observation that gaps appeared in the insulation with increasing operation time. Outliers in the results are mainly caused by varying ambient conditions like wind and ambient temperature.

a b

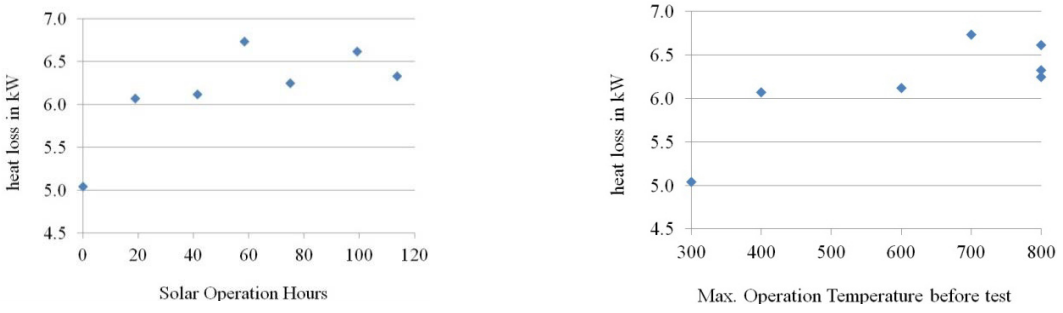

Fig. 9. (a) heat loss versus solar operation time; (b) heat loss versus maximum operating temperature

After the test period heat loss is calculated to be around 6.5kW at an average cavity temperature of 260°C and 15°C ambient temperature. With a surface area of the cavity $A_{surface}$ of about 21m² and a driving temperature difference of 245K the specific heat transfer coefficient $h_{insulation}$ is hence determined to be approximately 1.26W/m²*K using formula (2).

The conditions during these tests are far away from design point conditions in solar operation. For this reason heat loss of the system for design point conditions can only be estimated.

Therefore the higher driving temperature difference of 950K caused by air temperatures inside the cavity T_{inside} of approximately 1000°C and higher heat transfer coefficient $h_{insulation}$ at higher average temperature have to be considered. The heat transfer coefficient is unknown but depends mainly on the heat conductivity. As the heat conductivity of the used materials approximately doubles [8], the estimated heat loss results to be about 50kW.

$$Q_{heat\ loss} = A_{surface} * h_{insulation} * \left(T_{inside} - T_{outside}\right) \quad (2)$$

Thus, the heat loss of the prototype exceeds by far the target heat loss of 15kW.

5.3. Conclusion

The particular conditions of solar applications like inhomogeneous and fluctuating load led to an intolerable degradation of the chosen materials already after few hours of solar operation. The load case for insulation materials of solar applications seems to be more than just temperature. Where materials withstand high loads under homogenous and stationary condition they are not applicable to the required needs. Better solutions need to be found to handle shrinking and thermal expansion. The project showed clearly the demand for further research and long time experience in the field of commercial application for higher reliability and better performance. Further approaches like preshrinking and surface treatment of fiber materials, or applications of other materials like actively cooled metallic insulation, will be pursued.

Acknowledgements

This work was supported by Federal Ministry for the Environment, Nature Conservation, Building and Nuclear Safety (BMUB) based on a decision of the German Bundestag.

References

[1] Amsbeck, Lars and Denk, Thorsten and Ebert, Miriam and Gertig, Christian and Heller, Peter and Herrman, Patrik and Jedamski, Jens and John, Joachim and Tobias, Prosinečki and Rehn, Johnny (2010) Test of a solar-hybrid microturbine system and evaluation of storage deployment. Solarpaces 2010, 21.-24.Sep. 2010, Perpignan, Frankreich

[2] Quero, Dr., M. and Korzynietz, R. and Ebert, M. and Jiménez, A and del Río, A. and Brioso, J. (2013) Solugas – Operation experience of the first solar hybrid gas turbine system at MW scale. In: Solar PACES Conference (ISSN: 0199-6231). SolarPACES 2013, 17.-20. Sept. 2013, Las Vegas, USA. ISSN 0199-6231.

[3] Uhlig R., Flesch R., Gobereit B., Giuliano S., Liedke P. (2013) Strategies enhancing efficiency of cavity receivers. SolarPACES 2013, 17.-20. Sept. 2013, Las Vegas, USA

[4] Amsbeck, Lars and Buck, Reiner and Heller, Peter and Jedamski, Jens and Uhlig, Ralf (2008) Development of a tube receiver for a solar-hybrid microturbine system. SolarPaces 2008, 4.-7. March 2008, Las Vegas, USA

[5] Uhlig, Ralf (2011) Transient stresses at metallic solar tube receivers. SolarPaces 2011, 20. – 23. September 2011, Granada, Spain

[6] Amsbeck, Lars and Helsch, Gundula and Röger, Marc and Uhlig, Ralf (2009) Development of a Broadband Antireflection Coated Transparent Silica Window for a Solar-Hybrid Microturbine System. SolarPACES. SolarPACES 2009, 15.-18. September 2009, Berlin, Germany. ISBN 978-3-00-028755-8.

[7] Jedamski, Jens and Reiner, Buck and Heller, Peter and Uhlig, Ralf and Amsbeck, Lars and Couturier, Raphael and Tochon, Patrice and Vasquez, Felipe (2010) Development of a profiled multiplayer tube for high temperature solar receivers and heat exchangers. 14th International Heat Transfer Conference (IHTC 14), 08.-13. Aug. 2010, Washington D.C., USA.

[8] Data sheets SILCALOG WOOL 130-194 and SILCASTACK WOOL 130-18